Hindawi
Mathematical Problems in Engineering
Volume 2018, Article ID 2305187, 10 pages
https://doi.org/10.1155/2018/2305187

Research Article

Bifurcation Analysis of Stick-Slip Motion of the Vibration-Driven System with Dry Friction

Peng Li and Ziwang Jiang

School of Aerospace Engineering and Applied Mechanics, Tongji University, Shanghai 200092, China

Correspondence should be addressed to Peng Li; 1310548@tongji.edu.cn

Received 9 March 2018; Revised 26 June 2018; Accepted 12 August 2018; Published 27 August 2018

Academic Editor: Carlos Llopis-Albert

This paper is concerned with the vibration-driven system which can move due to the periodic motion of the internal mass and the dry friction; the system can be modeled as Filippov system and has the property of stick-slip motion. Different periodic solutions of stick-slip motion can be analyzed through sliding bifurcation, two-parameter numerical continuation for sliding bifurcation is carried out to get the different bifurcation curves, and the bifurcation curves divide the parameters plane into different regions which stand for different stick-slip motion of the periodic solution. Furthermore, continuations with additional condition $v = 0$ are carried out for the directional control of the vibration-driven system in one period; the curves divide the parameter plane into different progressions.

1. Introduction

Recently, mobile mechanisms that can move due to the vibration of the internal mass have been widely researched, and these mechanisms have many advantages over conventional mobile systems (driven by legs, wheels, wings, etc.), for example, easy fabrication, hermetic structure, and locomotion in the narrow environment. Thus they have extensive application in pipeline inspection, life detection in disaster, and medical endoscopy.

Chernousko [1] first proposed the horizontal motion of the system driven by the movable internal mass; the friction which acted on the body is anisotropic, which means the coefficient of friction in forward and backward direction is different. The two periodic control modes, velocity-controlled mode and acceleration-controlled mode, are constructed for the relative motion of the internal mass, and optimal parameters of periodic control were decided to realize the maximum mean velocity of the body. Fang et al. [2] used the method of averaging to obtain an approximate expression of the average steady-state velocity when the stick-slip phenomenon was not considered, optimal parameters of the internal controlled mass were determined to maximize the average velocity, and some control strategies were given to control the motion of system under the stick-slip effect. Liu et al. [3] studied the vibroimpact capsule system which has a main body interacting with an internal harmonically driven mass, when the internal mass contact with the plate impact occurs, and the parameters for the maximum mean velocity can be determined through nonlinear dynamics analysis, the energy consumption was also considered, and the parameters for the maximum mean velocity and the minimum energy consumption were not the same. Fang et al. [4, 5] and Zimmermann et al. [6–8] studied the two and more modules vibration-driven systems; the approximate expression of steady-state motion was obtained when the friction is small and the optimal parameters were got to achieve the maximum mean velocity. Bolotnik et al. [9] modeled the system driven by the movable internal mass which can move in the horizontal direction and the vertical direction (change the normal force for anisotropic friction in the different direction). Then the approximate expression of average steady-state velocity was obtained through the method of averaging; optimal parameters (the amplitude and the phase shift of the horizontal and vertical vibration excitation forces) were determined to realize the maximum average velocity and to control the direction of motion. In the paper, we study the model.

The dry friction plays an important role in vibration-driven system motion. The systems with dry friction belong to Filippov piecewise-smooth dynamical systems [10, 11]. The Filippov systems may exhibit different types of limit cycles caused by the interaction of a trajectory with the boundary of the sliding regions; the features of Filippov system are called the sliding bifurcation. Kowalczyk et al. [12] investigated a dry friction oscillator through numerical continuation of sliding bifurcation and revealed the codimension two sliding bifurcation points. Marcel Guardia et al. [13] analytically considered sliding bifurcations of periodic orbits in the dry friction oscillator, and the results agreed with the numerical calculation [12]. Fang et al. [14] studied the vibration-driven system through sliding bifurcation, and a two-parameter bifurcation problem was theoretically analyzed. For the numerical continuation of piecewise-smooth system, the software SlideCont [15] and TC-HAT [16] based on ATUO have been developed. Joseph Páez Chávez used the software TC-HAT to study the bifurcation of some mechanical models, the nonsmooth Jeffcott rotor [17], the impact oscillator [18], the piecewise-linear capsule system [19], etc. The continuation toolbox COCO was developed for continuation and bifurcation analysis of smooth and nonsmooth dynamical systems [20, 21]; the soft impact oscillator [22] and the impulsively coupled oscillators [23] were analyzed through the COCO. In this paper, the COCO will be employed to numerically study the sliding bifurcation of vibration-driven system; the sliding bifurcation will help us to understand the stick-slip property of periodic solution and give some instructive ideas to design and control the system.

The paper is organized as follows. In Section 2, the model of the vibration-driven system is described. The mathematical model of vibration-driven system is studied in detail in order to perform the numerical analysis by the mean of COCO in Section 3. Two-parameter sliding bifurcations are analyzed and the directional control of the vibration-driven system is tackled by the numerical continuation in Section 4, and some conclusions are given in Section 5.

2. Modeling of Vibration-Driven System

The vibration-driven system is considered as depicted in Figure 1. The vibration-driven system is composed of a rigid body and an internal mass; the rigid body realizes the translational motion along a straight line in the resistive environment. The internal mass can move relative to the rigid body in horizontal and vertical direction. The internal mass is considered a point mass. Dry friction acts between the rigid body and the ground.

Two Cartesian reference frames are introduced: the inertial reference frame Oxy and the coordinate system $O'\xi\eta$ attached to the rigid body. The x- and ξ-axes are horizontal; the y– and η-axes are vertical. We denote x as the coordinate of the point O' in the inertial reference frame Oxy, x denotes the displacement of the rigid body, ξ and η denote the coordinates of the internal body in the reference frame $O'\xi\eta$, m and m_1 are the masses of the rigid body and the internal body, respectively, and g is the gravitational acceleration.

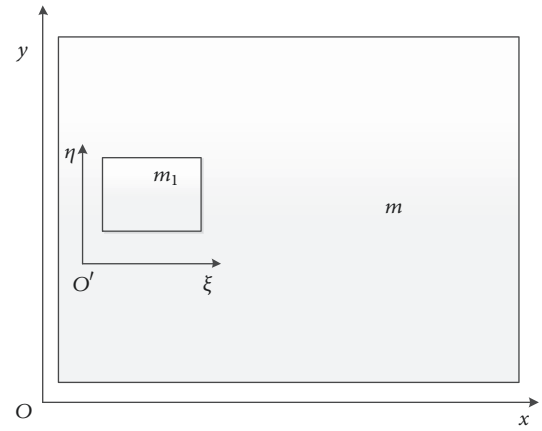

Figure 1: Vibration-driven system.

The dynamics equation of the system along x–axis can be governed by Newton's second laws as follows:

$$(m + m_1)\ddot{x} + m_1\ddot{\xi} = F_f, \tag{1}$$

where F_f is the frictional force. The force F_f is described by Coulomb law:

$$F_f = \begin{cases} -\mu F_N \operatorname{sgn} \dot{x}, & if\ \dot{x} \neq 0, \\ -F_0, & if\ \dot{x} = 0 \& |F_0| \leq \mu F_N, \\ -\mu F_N \operatorname{sgn} F_0, & if\ \dot{x} = 0 \& |F_0| > \mu F_N, \end{cases} \tag{2}$$

where F_0 is the resultant force on the body except for the dry friction in the horizontal direction, F_N is the normal force exerted on the system by the ground, and μ is the coefficient of dry friction. The asymmetrical friction in forward and backward motions arises from the time-varying normal force F_N. The force F_0 and force F_N can be expressed:

$$F_0 = -m_1\ddot{\xi}, \tag{3}$$

$$F_N = (m + m_1)g + m_1\ddot{\eta}. \tag{4}$$

The rigid body keeps the contact with the ground; therefore, the force F_N must be satisfied the inequality $F_N \geq 0$. So we have

$$(m + m_1)g + m_1\ddot{\eta} \geq 0. \tag{5}$$

Next, we assume the control acceleration is harmonic function with the same frequency but shifted in the phase; particularly,

$$\begin{aligned} \ddot{\xi} &= -A \sin \omega t, \\ \ddot{\eta} &= B \sin(\omega t + \phi). \end{aligned} \tag{6}$$

Here A and B are the driving-amplitudes, respectively, ω is the driving-frequency, and ϕ is the phase difference between the forces.

Substituting (6) into (1)-(5),

$$M\ddot{x} = F_x \sin \omega t + F_f, \tag{7}$$

$$F_f = \begin{cases} -\mu F_N \operatorname{sgn} \dot{x}, & if\ \dot{x} \neq 0, \\ -F_x \sin \omega t, & if\ \dot{x} = 0 \& \left|F_x \sin \omega t\right| \leq \mu F_N, \\ -\mu F_N \operatorname{sgn} \sin \omega t, & if\ \dot{x} = 0 \& \left|F_x \sin \omega t\right| > \mu F_N, \end{cases} \tag{8}$$

$$F_N = Mg + F_y \sin\left(\omega t + \phi\right), \quad F_N \geq 0, \tag{9}$$

where $M = m + m_1$, $F_x = m_1 A$, and $F_y = m_1 B$.

To reduce the number of parameters of the system, the nondimensional variables x^* and t^* and the parameters ε and α are introduced:

$$\begin{aligned} x^* &= \frac{M\omega^2}{F_x} x, \\ t^* &= \omega t, \\ \varepsilon &= \mu \frac{Mg}{F_x}, \\ \alpha &= \frac{F_y}{Mg} \end{aligned} \tag{10}$$

Substituting these variables above into (7)-(9) (omit the asterisks),

$$\ddot{x} = \sin t + f_c, \tag{11}$$

$$f_c = \begin{cases} -\varepsilon f_n \operatorname{sgn} \dot{x}, & if\ \dot{x} \neq 0, \\ -\sin t, & if\ \dot{x} = 0 \& |\sin t| \leq \varepsilon f_n, \\ -\varepsilon f_n \operatorname{sgn}\ \sin t, & if\ \dot{x} = 0 \& |\sin t| > \varepsilon f_n, \end{cases} \tag{12}$$

$$f_n = 1 + \alpha \sin\left(t + \phi\right), \quad \alpha \leq 1. \tag{13}$$

The expressions f_c and f_n stand for the normalized dry friction and the normal force, respectively. The parameter ε represents the ratio of the possible maximum value of the dry friction force to the amplitude F_x. We assume the value of the parameter ε is in the interval $(0, 1)$. Due to periodicity, the phase difference ϕ ranges from 0 to 2π.

3. Modeling of the Vibration-Driven System as Filippov System

The mathematical model of vibration-driven system can be defined as a piecewise-smooth system of the Filippov type. We can transform (11) into vector fields, event functions, and reset functions through the approach of multisegment periodic orbits. Let $\mathbf{y} = (y_1, y_2)^T = (\dot{x}, t)^T$ and $\mathbf{p} = (\varepsilon, \alpha, \phi)^T$ represent the state variables of the system and the parameters, respectively.

The multisegment periodic orbits of the vibration-driven system consist of two or more segments, which can be modeled as follows.

Stick: This segment occurs when $\sin y_2 < |\varepsilon f_n|$; the motion during this segment is governed by the equation

$$\dot{\mathbf{y}} = f_s = \begin{pmatrix} 0 \\ 1 \end{pmatrix}. \tag{14}$$

This segment terminates when the resultant force on the body except for the dry friction equals the threshold of the dry friction force. The event functions are detected as follows:

$h_f(\mathbf{y}) = \sin y_2 - \varepsilon(1 + \alpha \sin(y_2 + \phi)) = 0$ (transition to forward slip)

$h_b(\mathbf{y}) = \sin y_2 + \varepsilon(1 + \alpha \sin(y_2 + \phi)) = 0$ (transition to backward slip)

The next segment initial point is defined by the reset function $g_{id}(\mathbf{y}) = \mathbf{y}$.

Forward slip: this segment occurs when the force is larger than the maximum value of the dry friction; that is, $\sin y_2 > \varepsilon(1 + \alpha \sin(y_2 + \phi))$; the motion during this segment is governed by the equation

$$\dot{\mathbf{y}} = f_f = \begin{pmatrix} \sin y_2 - \varepsilon\left(1 + \alpha \sin\left(y_2 + \phi\right)\right) \\ 1 \end{pmatrix}. \tag{15}$$

This segment ends when the velocity becomes zero; that is, $h(\mathbf{y}) = y_1 = 0$. The next segment is connected by the reset function $g_{id}(\mathbf{y}) = \mathbf{y}$.

Backward slip: this segment occurs when $\sin y_2 < -\varepsilon(1 + \alpha \sin(y_2 + \phi))$; the motion of the system during this segments is described by the equation

$$\dot{\mathbf{y}} = f_b = \begin{pmatrix} \sin y_2 + \varepsilon\left(1 + \alpha \sin\left(y_2 + \phi\right)\right) \\ 1 \end{pmatrix}. \tag{16}$$

This segment ends when the velocity becomes zero; the event function is defined: $h(\mathbf{y}) = y_1 = 0$. The next segment is connected by the reset function $g_{id}(\mathbf{y}) = \mathbf{y}$.

Stick 2π: this segment is introduced to keep the variable y_2 within the interval $[0, 2\pi)$, when $\sin y_2 < |\varepsilon f_n|$, the motion of the system is governed by (14), the segment ends when $h_{2\pi}(\mathbf{y}) = 2\pi - y_2 = 0$, and the reset function is

$$g_{2\pi}\left(\mathbf{y}\right) = \begin{pmatrix} y_1 \\ y_2 - 2\pi \end{pmatrix}. \tag{17}$$

Forward slip 2π: this segment is introduced to keep the variable y_2 within the interval $[0, 2\pi)$, when $\sin y_2 > \varepsilon(1 + \alpha \sin(y_2 + \phi))$, the motion of the system is governed by (15), the segment ends when $h_{2\pi}(\mathbf{y}) = 2\pi - y_2 = 0$, and the reset function is $g_{2\pi}(\mathbf{y})$.

Backward slip 2π: this segment is introduced to keep the variable y_2 within the interval$[0, 2\pi)$, when $\sin y_2 < -\varepsilon(1 + \alpha \sin(y_2 + \phi))$, the motion of the system is governed by (16), the segment ends when $h_{2\pi}(\mathbf{y}) = 2\pi - y_2 = 0$, and the reset function is $g_{2\pi}(\mathbf{y})$.

A periodic solution of Filippov system can be described as a sequence of triplet $I_i = (f_i, h_i, g_i)$; the segment of system is governed by the vector field f_i, terminates at the

event function h_i, and connects the next segment by the reset function g_i. Any periodic trajectory of the system is described by solution signature $\{I_i\}_{i=1}^{M}$; M is the length of signature. Therefore the periodic solution of the vibration-driven can be described by combinations of the seven triplets corresponding to above statement:

$$\begin{aligned} I_1 &= \left(f_s, h_f, g_{id}\right), \\ I_2 &= \left(f_s, h_b, g_{id}\right), \\ I_3 &= \left(f_f, h, g_{id}\right), \\ I_4 &= \left(f_b, h, g_{id}\right), \\ I_5 &= \left(f_s, h_{2\pi}, g_{2\pi}\right), \\ I_6 &= \left(f_f, h_{2\pi}, g_{2\pi}\right), \\ I_7 &= \left(f_b, h_{2\pi}, g_{2\pi}\right). \end{aligned} \tag{18}$$

In the Filippov system, there are four possible sliding bifurcations in the limit cycle because of the interaction of a trajectory with the boundary of a sliding region, including crossing-sliding bifurcation, gazing-sliding bifurcation, switching-sliding bifurcation, and adding-sliding bifurcation. Nondegeneracy conditions for the four sliding bifurcation are given [10, 11]. The sliding bifurcation does not change the number and stability of the system's solutions, but it will induce the different interaction between the limit cycle and the sliding regions.

4. Numerical Bifurcation Analysis

In this section, we will perform the sliding bifurcation and directional control to analyze the dynamics response of the vibration-driven system.

4.1. Sliding Bifurcation Analysis. When $\varepsilon = 0.6, \alpha = 0.456, \phi = 2\pi/3$, the periodic trajectory of the motion is shown by Figure 2. The cycle signature is $\{I_1, I_3, I_4, I_5\}$. We start the numerical continuation of the periodic solution by the method of path-following using the parameter value as an initial value. The additional boundary $h_b(\mathbf{y}) = \sin y_2 + \varepsilon(1 + \alpha \sin(y_2+\phi)) = 0$ may be applied to the start point of the third segment for the crossing-sliding bifurcation continuation. We will use the COCO to carry out the numerical continuation concerning parameters ϕ and ε; the curve cs_1 which is the result of this numerical continuation is shown in Figure 3.

Similarly, the numerical continuation is performed in parameter space $\phi \times \varepsilon$ with different cycle signatures and different additional boundary condition for different segment boundary point and the results are depicted in Figure 3. The signature of cycle trajectory in E_1 is $\{I_1, I_3, I_5\}$, when the additional conditions $h_b(\mathbf{y}) = \sin y_2 + \varepsilon(1 + \alpha \sin(y_2 + \phi)) = 0$ and $\cos y_2 + \varepsilon\alpha \cos(y_2 + \phi) = 0$ are applied to the point of the segment I_5 according to nondegeneracy conditions of adding-sliding bifurcation; hence we can get the adding-sliding bifurcation curve ad_1. The adding-sliding bifurcation

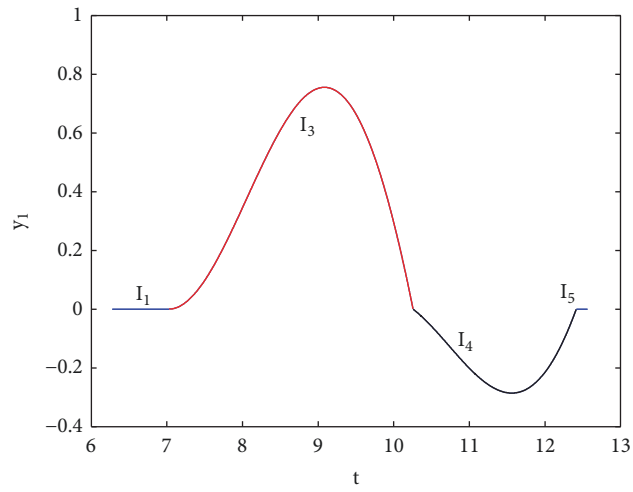

Figure 2: Periodic solution of vibration-driven system (11) computed for the parameter values $\varepsilon = 0.6$, $\alpha = 0.456$, $\phi = 2\pi/3$. The trajectory consists of the segments I_1, I_3, I_4, I_5.

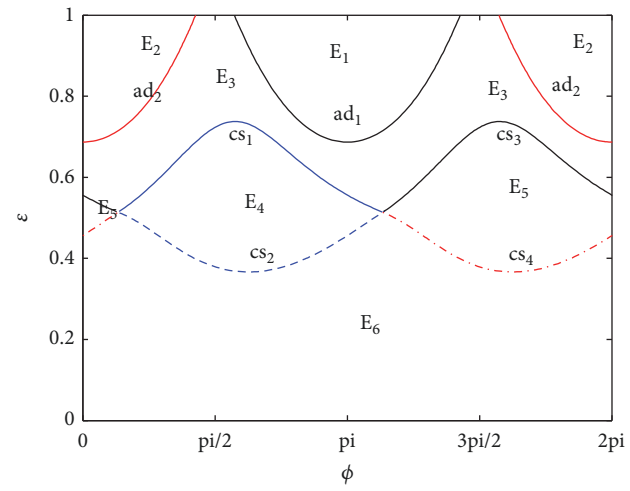

Figure 3: Two-parameter continuation of sliding bifurcation with respect to ϕ and ε for $\alpha = 0.456$. ad_i represent adding-sliding bifurcations, cs_i represent crossing-sliding bifurcations, and the regions E_i denote the different stick-slip motions of the periodic solutions.

branch ad_2 is got similarly. The curves cs_1, cs_2, cs_3, and cs_4 represent crossing-sliding bifurcation branches. The sliding bifurcation curves divide the two parameters plane into eight regions and there are six different stick-slip periodic solutions in the parameter plane. The periodic solution of system in E_1 with signature $\{I_1, I_3, I_5\}$ is depicted in Figure 4(a), which means the velocity of the system is always greater than or equal to 0. The signature of the periodic trajectory in E_2 is $\{I_4, I_2, I_7\}$ as depicted in Figure 4(b), which means the velocity of the system is always lower than or equal to 0. The velocity in the two regions does not change its sign; it is important for the practical application to do some work, such as medical robot for intestinal therapy. Furthermore, when the velocity of system changes its sign, the efficiency will decrease because

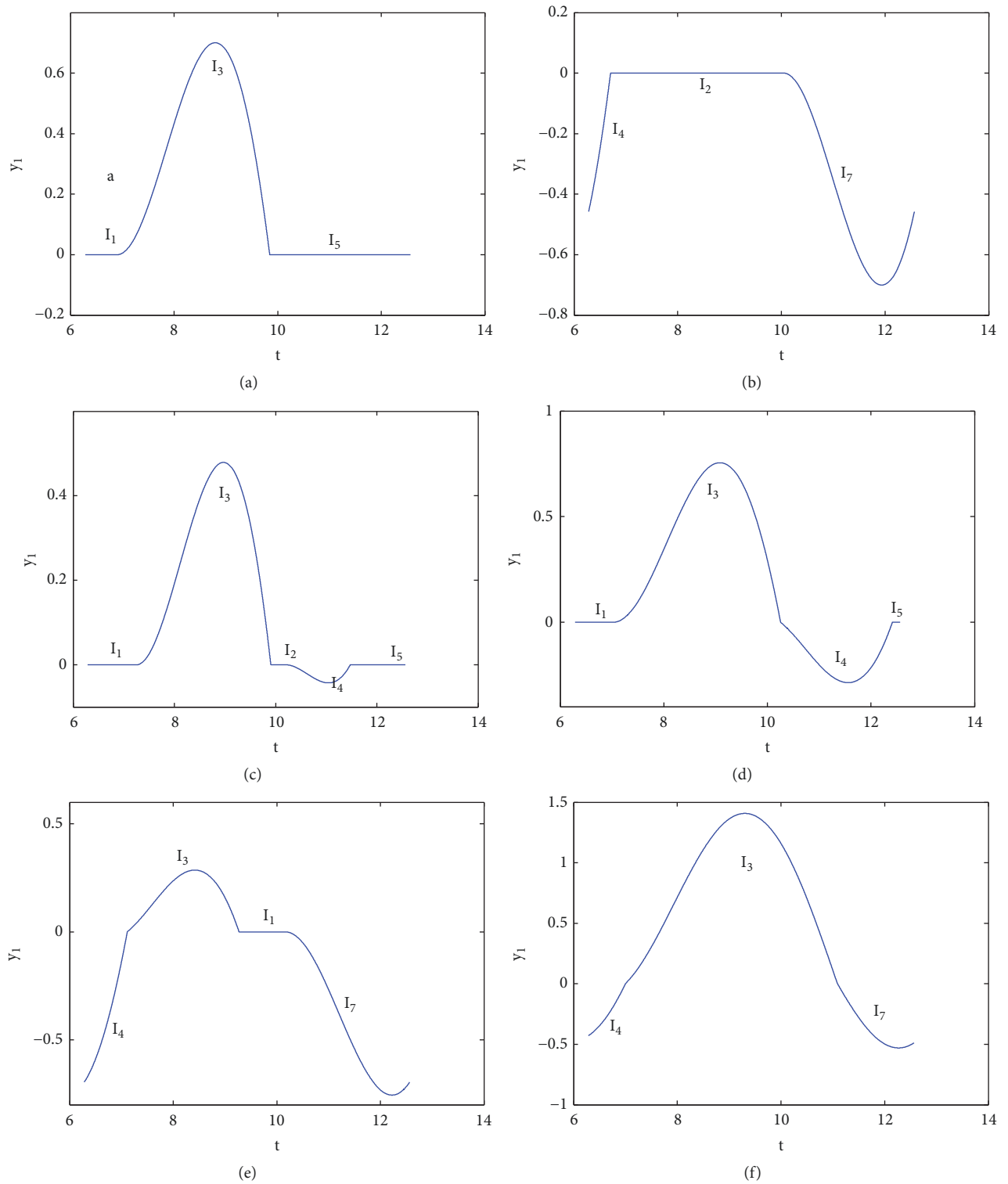

FIGURE 4: The velocity of the vibration-driven system for $\alpha = 0.456$, (a) $\varepsilon = 0.8$, $\phi = \pi$ in E_1. (b) $\varepsilon = 0.8$, $\phi = 0$ in E_2. (c) $\varepsilon = 0.8$, $\phi = 2\pi/3$ in E_3. (d) $\varepsilon = 0.6$, $\phi = 2\pi/3$ in E_4. (e) $\varepsilon = 0.6$, $\phi = 5\pi/3$ in E_5. (f) $\varepsilon = 0.2$, $\phi = 2\pi/3$ in E_6.

of more energy dissipated by opposite slip. The limit cycle of system in E_3 can be described by the signature $\{I_1, I_3, I_2, I_4, I_5\}$ depicted in Figure 4(c). The signature of periodic solution in E_4 is $\{I_1, I_3, I_4, I_5\}$ showed in Figure 4(d); the signature of the periodic solution in E_5 is $\{I_4, I_3, I_1, I_7\}$ depicted in Figure 4(e). The cyclic signature in Figure 4(f) is $\{I_4, I_3, I_7\}$.

The result of two-parameter continuation for the sliding bifurcation with respect to the parameters ϕ and ε by fixing

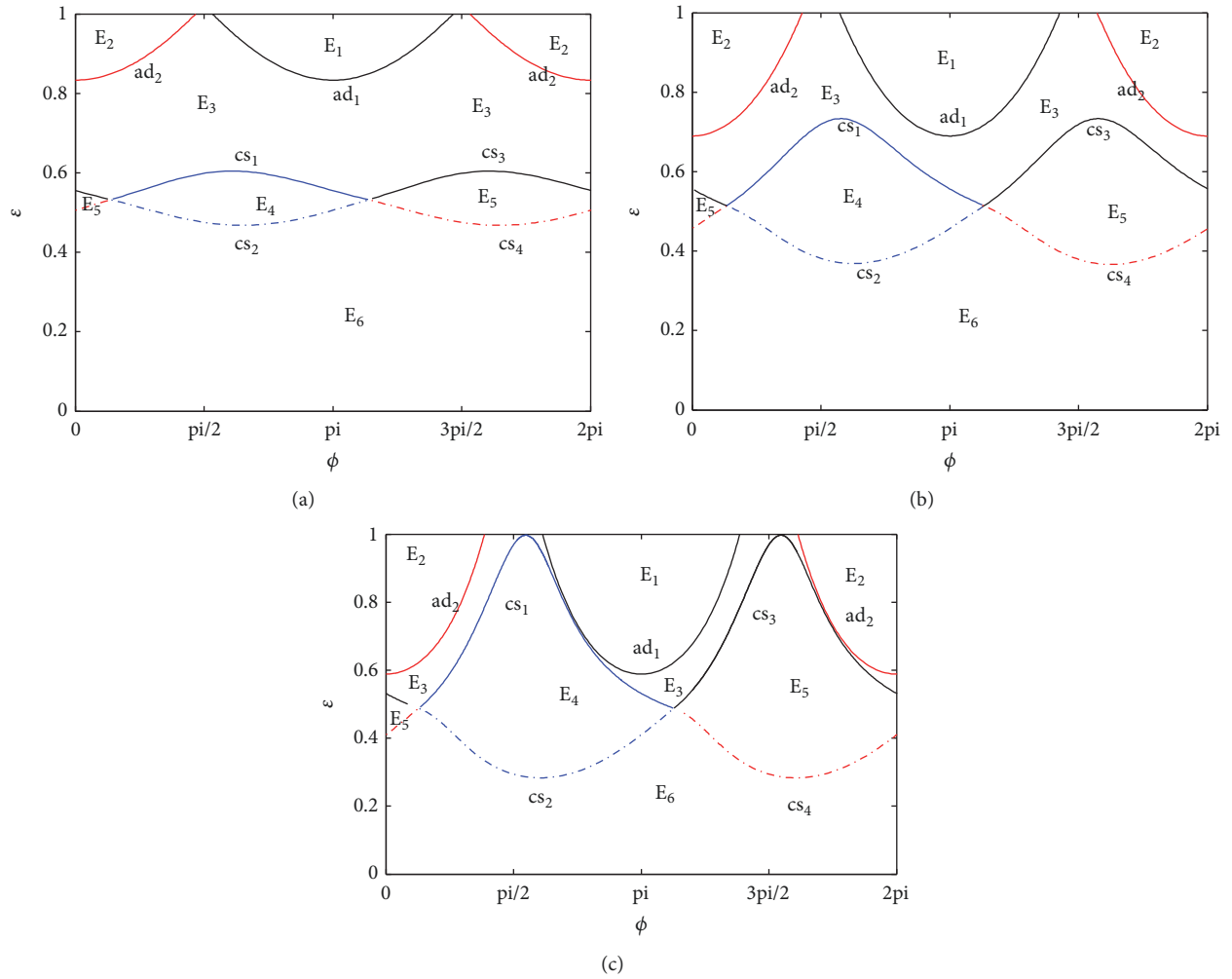

Figure 5: Two-parameter continuations of sliding bifurcation with respect to ϕ and ε for different parameter α: (a) $\alpha = 0.2$; (b) $\alpha = 0.45$; (c) $\alpha = 0.7$; ad_i represent adding-sliding bifurcations, cs_i represent crossing-sliding bifurcations, and the regions E_i denote the different stick-slip motions of the periodic solutions.

different value α ((a) $\alpha = 0.2$; (b) $\alpha = 0.45$; (c) $\alpha = 0.7$) is shown in Figure 5. The regions E_3 and E_6 are shrinking and the regions E_1, E_2, E_4, and E_5 are expanding as the α increases. Therefore it is easy to realize directional motion in E_1 or E_2 through changing the parameters when the parameter α increases.

We carry out the numerical continuation with respect to the parameters ε, α in $[0, 1] \times [0, 1]$ for the different ϕ and the results are depicted in Figure 6 ((a) $\phi = \pi/3$; (b) $\phi = 2\pi/3$; (c) $\phi = 4\pi/3$). The periodic solutions in region E_i in Figures 3 and 6 have the same stick-slip motion; the curve ss_1 represents the switching-sliding bifurcation branch. As shown from Figure 6, there are different regions of stick-slip motion of system in the parameter plane when ϕ is different; the motion in E_2 which is always equal to or lower than 0 can be realized by changing the parameter ε and α when $\phi = \pi/3$, but the motion in E_1 could not happen no matter the value of ε and α. The velocity of system which is always equal to or larger than zero can be controlled through changing the parameter when ϕ is $2\pi/3$ or $4\pi/3$. Therefore the value of ϕ is important for realizing directional motion.

The numerical continuation for the parameters ϕ, α in the $[0, 2\pi] \times [0, 1]$ by fixing the value of the parameter ε is carried out and the results are depicted in Figure 7. From Figure 7, there are no regions E_1 and E_2 in the parameter plane when $\varepsilon = 0.4$, but the regions E_1 and E_2 appear in the parameter plane as ε increases to 0.6; the regions E_1 and E_2 expand when $\varepsilon = 0.8$.

4.2. Directional Control. Based on the above analysis, we can see that the direction of the system progression in one period can be forward (the region E_1 in Figure 3) or backward (the region E_2 in Figure 3) owing to different parameters.

The average velocity of the system in one period is

$$v = \frac{1}{T} \int_0^T y_1(t)\, dt. \tag{19}$$

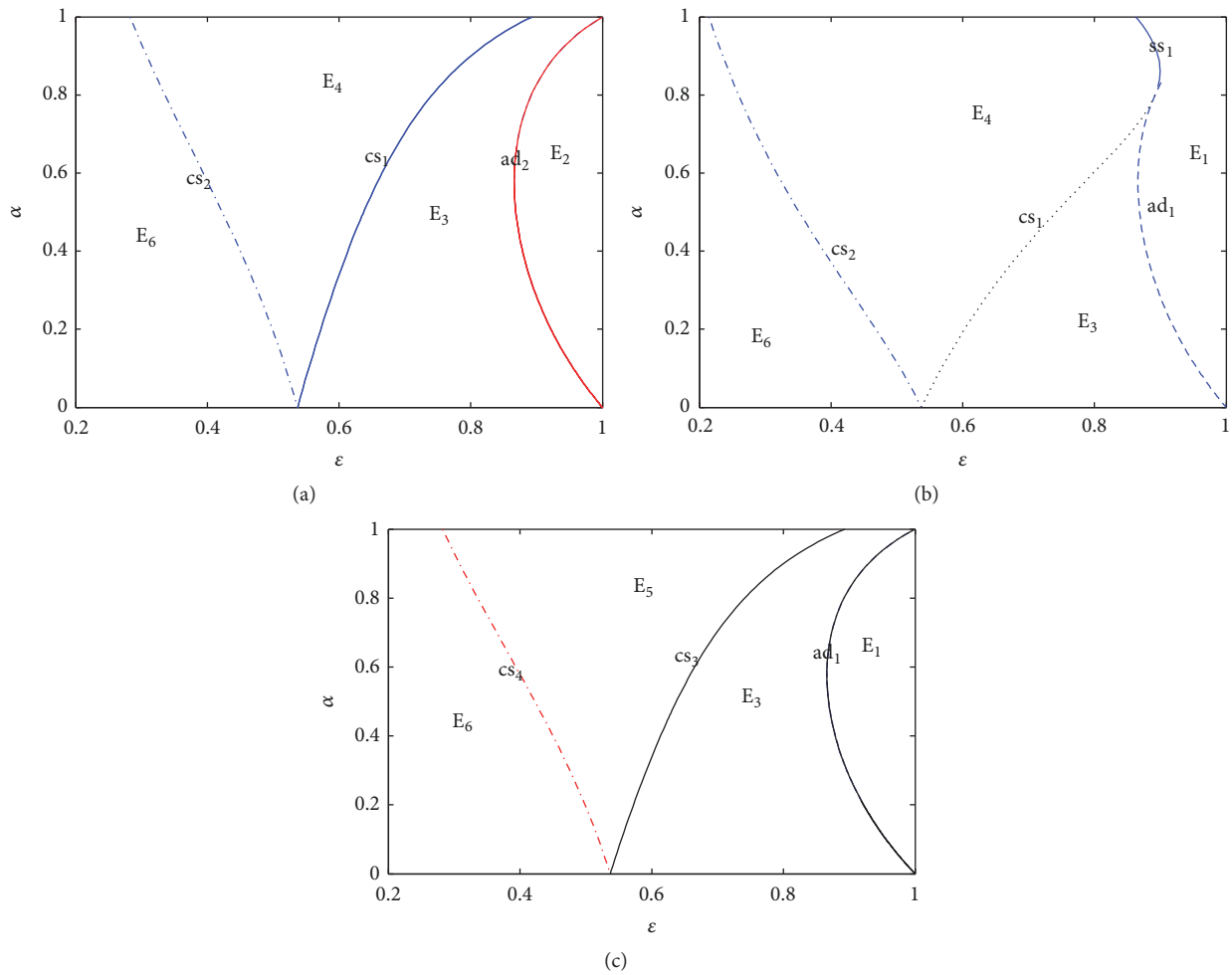

FIGURE 6: Two-parameter continuation of sliding bifurcation with respect to ε and α for different ϕ: (a) $\phi = \pi/3$; (b) $\phi = 2\pi/3$; (c) $\phi = 4\pi/3$; ad_i represent adding-sliding bifurcations, cs_i represent crossing-sliding bifurcations, ss_i represent switching-sliding bifurcations, and the regions E_i denote the different stick-slip motions of the periodic solutions.

The regions of different directional progression in one period can be determined by implementing the parameters continuation of the periodic solution with additional condition $v = 0$.

When $\alpha = 0.456$, there are six different stick-slip period solutions in the parameter plane in Figure 3; two parameters ϕ, ε can be continued numerically based on different period solutions with the additional condition $v = 0$. The result is presented in Figure 8. The curves divide the parameters into three regions: forward drift ($v > 0$), backward drift ($v < 0$), and zero drift ($v = 0$, on the curves). They are shown in Figures 9(a), 9(b), and 9(c), respectively. According to Figure 8, it can be seen that, for any value of the parameter ε, the direction of system progression can be controlled by changing the phase ϕ, the direction of progression is forward when ϕ is in $(\pi/2, \pi)$, and the direction of progression is backward when ϕ is in $(3\pi/2, 2\pi)$. When $0.7239 < \varepsilon < 1$, the direction of progression is forward when ϕ is in $(\pi/2, 3\pi/2)$; and the direction of progression is backward when ϕ is in $(0, \pi/2)$ and $(3\pi/2, 2\pi)$.

When $\phi = 2\pi/3$, there is no solution with additional condition $v = 0$ in the parameter $\varepsilon - \alpha$ plane, which indicates that the direction of the progression does not change. The direction of the progression is forward because the average velocity is larger than zero in the region E_1 seen from Figure 6(b).

When $\varepsilon = 0.6$, the parameter ϕ-α plane for directional continuation is presented in Figure 10, some conclusions are draw from Figure 10 similarly: for any parameter α, the direction of system progression can be controlled by changing the phase ϕ; the direction of progression is forward when ϕ is in $(\pi/2, 4.4211)$; and the direction of progression is backward when ϕ is in $(3\pi/2, 2\pi)$ and $(0, 1.2795)$. When $0 < \alpha < 0.2278$, the direction of progression is forward when ϕ is in $(\pi/2, 3\pi/2)$; and the direction of progression is backward when ϕ is in $(0, \pi/2)$ and $(3\pi/2, 2\pi)$.

5. Conclusions

This paper studies the dynamical response of the vibration-driven system which is composed of a body with movable internal mass. The asymmetry of friction in forward and backward direction is essential to the motion of system,

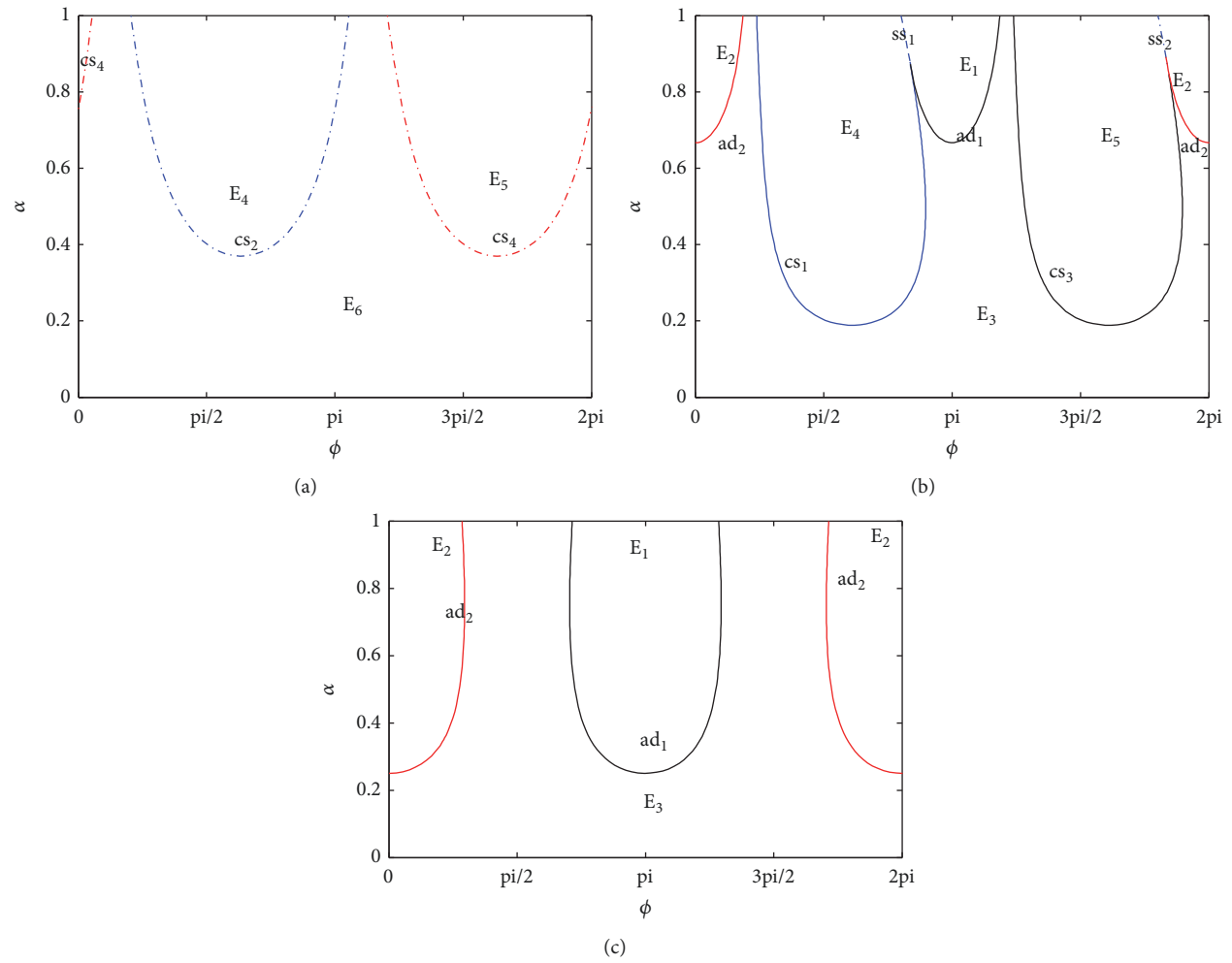

FIGURE 7: Two-parameter continuation of sliding bifurcation with respect to ϕ and α for different ε: (a) $\varepsilon = 0.4$; (b) $\varepsilon = 0.6$; (c) $\varepsilon = 0.8$; ad_i represent adding-sliding bifurcations, cs_i represent crossing-sliding bifurcations, ss_i represent switching-sliding bifurcations, and the regions E_i denote the different stick-slip motions of the periodic solutions.

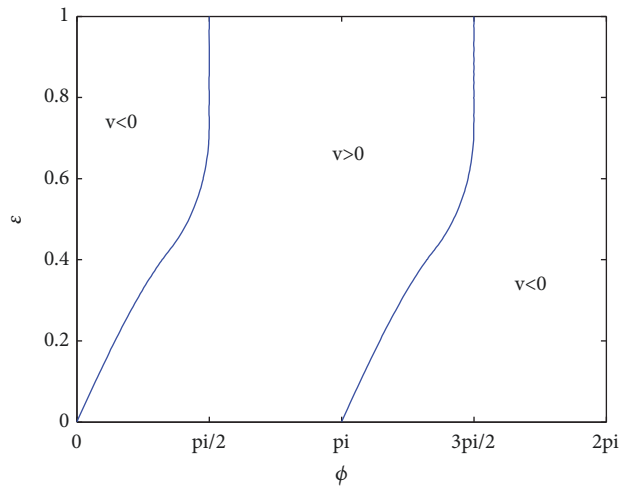

FIGURE 8: Two-parameter continuations of the periodic orbits for the parameter $\alpha = 0.456$. The average velocity is zero along the curves in the plane.

which arises from the normal force change due to the vertical motion of the internal mass. The vibration-driven system involving dry friction belongs to the Filippov system, the cycle trajectory of the system can be divided into smooth segments, the event functions defined the terminal point of the segments, and the reset functions connected the segments. We take advantage of the software COCO to carry out the bifurcation analysis.

Two-parameter sliding bifurcations are carried out by performing the numerical continuation. Different period solutions of stick-slip motion are obtained though the sliding bifurcation curves. For directional control of the vibration-driven system, the drift of the vibration-driven system in one period may change sign, the continuation with additional condition $v = 0$ is carried out in the parameters plane, and the curves are obtained. The curves divide the parameters plane into three modes of drift (backward, forward, and zero). So the direction of the vibration-driven system progression can be controlled by changing the parameters.

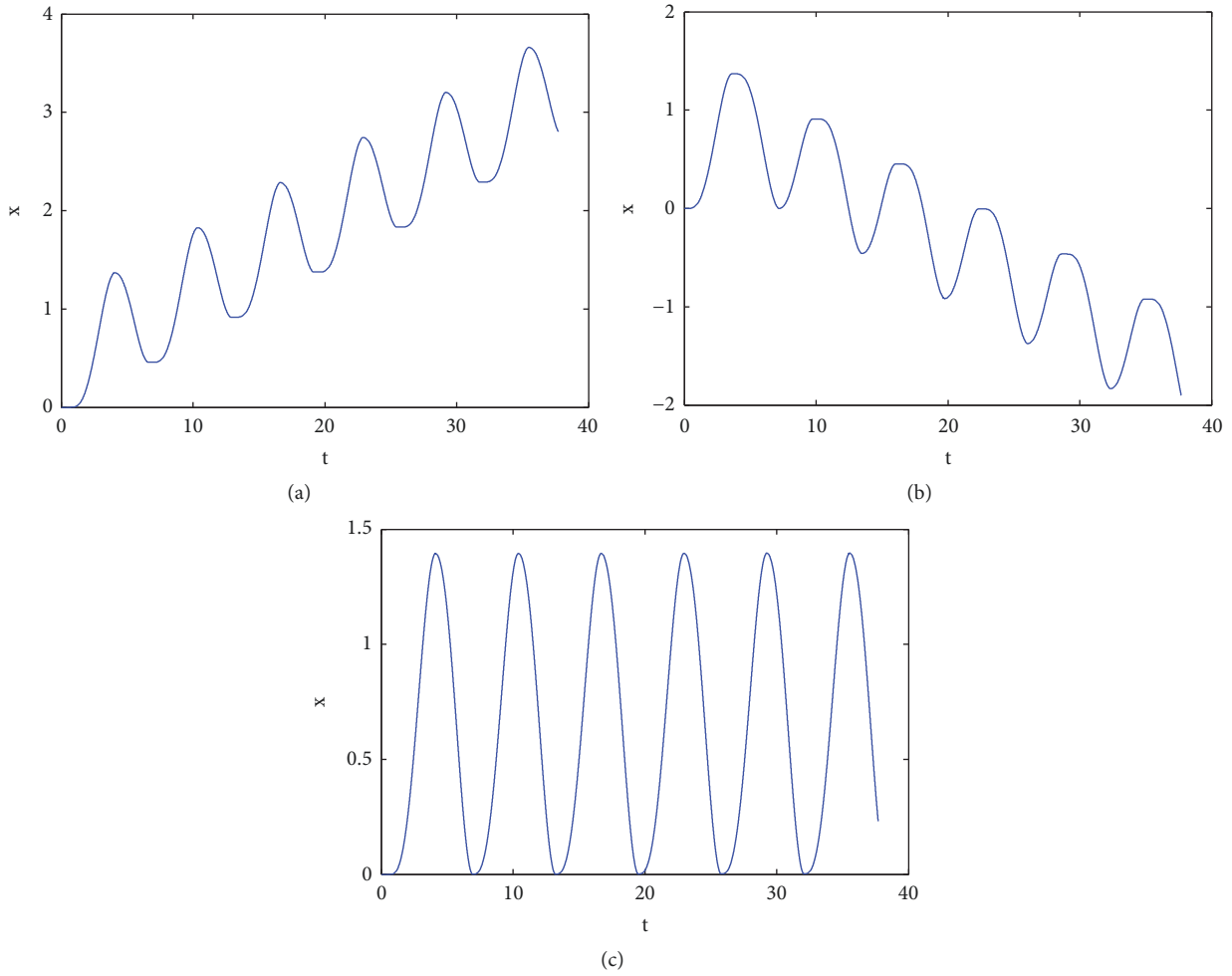

Figure 9: The progression of the vibration-driven system for (a) $\varepsilon = 0.5$, $\alpha = 0.456$, $\phi = \pi/2$; (b) $\varepsilon = 0.5$, $\alpha = 0.456$, $\phi = 3\pi/2$; (c) $\varepsilon = 0.4271$, $\alpha = 0.456$, $\phi = 1.1121$.

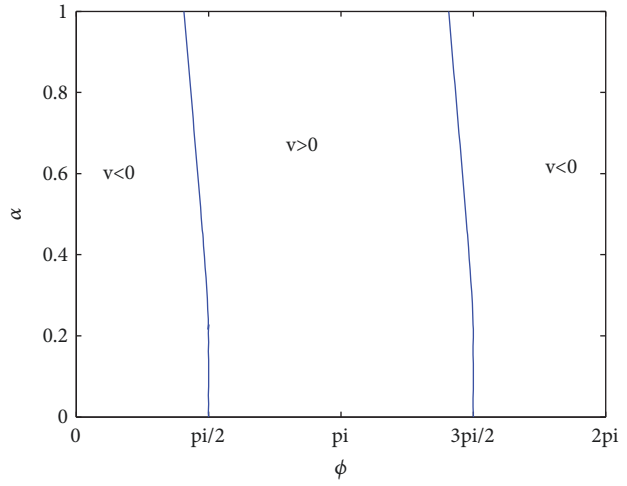

Figure 10: Two-parameter continuation of the periodic orbits for the parameter $\varepsilon = 0.6$. The average velocity is zero along the curves in the plane.

The particular contribution of this research is the numerical continuation of the parameters for the vibration-driven system and detailed classifications of parameter space where different system dynamic behaviors can be obtained. The bifurcation analysis improves our understanding of the dynamical behaviors of the vibration-driven system and is of benefit to devise control strategies for the vibration-driven system.

Data Availability

No data were used to support this study.

Disclosure

The research did not receive specific funding.

Conflicts of Interest

The authors declare that they have no conflicts of interest.

References

[1] F. L. Chernous'ko, "Analysis and optimization of the motion of a body controlled by means of a movable internal mass," *Journal of Applied Mathematics and Mechanics*, vol. 70, no. 6, pp. 819–842, 2006.

[2] H.-B. Fang and J. Xu, "Dynamics of a mobile system with an internal acceleration-controlled mass in a resistive medium," *Journal of Sound and Vibration*, vol. 330, no. 16, pp. 4002–4018, 2011.

[3] Y. Liu, M. Wiercigroch, E. Pavlovskaia, and H. Yu, "Modelling of a vibro-impact capsule system," *International Journal of Mechanical Sciences*, vol. 66, pp. 2–11, 2013.

[4] H.-B. Fang and J. Xu, "Controlled motion of a two-module vibration-driven system induced by internal acceleration-controlled masses," *Archive of Applied Mechanics*, vol. 82, no. 4, pp. 461–477, 2012.

[5] H.-b. Fang and J. Xu, "Dynamics of a three-module vibration-driven system with non-symmetric Coulomb's dry friction," *Multibody System Dynamics*, vol. 27, no. 4, pp. 455–485, 2012.

[6] K. Zimmermann, I. Zeidis, and C. Behn, *Mechanics of Terrestrial Locomotion: With a Focus on Non-pedal Motion Systems*, Springer, Heidelberg, Germany, 2009.

[7] K. Zimmermann, I. Zeidis, N. Bolotnik, and M. Pivovarov, "Dynamics of a two-module vibration-driven system moving along a rough horizontal plane," *Multibody System Dynamics*, vol. 22, no. 2, pp. 199–219, 2009.

[8] K. Zimmermann, I. Zeidis, M. Pivovarov, and C. Behn, "Motion of two interconnected mass points under action of non-symmetric viscous friction," *Archive of Applied Mechanics*, vol. 80, no. 11, pp. 1317–1328, 2010.

[9] N. N. Bolotnik, I. M. Zeidis, K. Zimmermann, and S. F. Yatsun, "Dynamics of controlled motion of vibration-driven systems," *Journal of Computer and Systems Sciences International*, vol. 45, no. 5, pp. 831–840, 2006.

[10] Y. A. Kuznetsov, S. Rinaldi, and A. Gragnani, "One-parameter bifurcations in planar Filippov systems," *International Journal of Bifurcation and Chaos*, vol. 13, no. 8, pp. 2157–2188, 2003.

[11] M. Bernardo, C. Budd, A. R. Champneys, and P. Kowalczyk, *Piecewise-Smooth Dynamical Systems: Theory And Applications*, Springer, Berlin, Germany, 2008.

[12] P. Kowalczyk and P. T. Piiroinen, "Two-parameter sliding bifurcations of periodic solutions in a dry-friction oscillator," *Physica D: Nonlinear Phenomena*, vol. 237, no. 8, pp. 1053–1073, 2008.

[13] M. Guardia, S. J. Hogan, and T. M. Seara, "An analytical approach to codimension-2 sliding bifurcations in the dry-friction oscillator," *SIAM Journal on Applied Dynamical Systems*, vol. 9, no. 3, pp. 769–798, 2010.

[14] H. Fang and J. Xu, "Stick-Slip Effect in a Vibration-Driven System With Dry Friction: Sliding Bifurcations and Optimization," *Journal of Applied Mechanics*, vol. 81, no. 5, p. 051001, 2013.

[15] F. Dercole and Y. A. Kuznetsov, "SlideCont: an Auto97 driver for bifurcation analysis of Filippov systems," *ACM Transactions on Mathematical Software*, vol. 31, no. 1, pp. 95–119, 2005.

[16] P. Thota and H. Dankowicz, "TC-HAT: A Novel Toolbox for the Continuation of Periodic Trajectories in Hybrid Dynamical Systems," *SIAM Journal on Applied Dynamical Systems*, vol. 7, no. 4, pp. 1283–1322, 2008.

[17] J. Páez Chávez and M. Wiercigroch, "Bifurcation analysis of periodic orbits of a non-smooth Jeffcott rotor model," *Communications in Nonlinear Science and Numerical Simulation*, vol. 18, no. 9, pp. 2571–2580, 2013.

[18] J. Páez Chávez, E. Pavlovskaia, and M. Wiercigroch, "Bifurcation analysis of a piecewise-linear impact oscillator with drift," *Nonlinear Dynamics*, vol. 77, no. 1-2, pp. 213–227, 2014.

[19] J. Páez Chávez, Y. Liu, E. Pavlovskaia, and M. Wiercigroch, "Path-following analysis of the dynamical response of a piecewise-linear capsule system," *Communications in Nonlinear Science and Numerical Simulation*, vol. 37, pp. 102–114, 2016.

[20] H. Dankowicz and F. Schilder, "An Extended Continuation Problem for Bifurcation Analysis in the Presence of Constraints," *Journal of Computational and Nonlinear Dynamics*, vol. 6, no. 3, 2011.

[21] H. Dankowicz and F. Schilder, *Recipes for continuation*, Society for Industrial and Applied Mathematics, Philadelphia, Pennsylvania, 2013.

[22] H. Jiang and M. Wiercigroch, "Geometrical insight into non-smooth bifurcations of a soft impact oscillator," *IMA Journal of Applied Mathematics*, vol. 81, no. 4, pp. 662–678, 2016.

[23] H. Jiang, Y. Liu, L. Zhang, and J. Yu, "Anti-phase synchronization and symmetry-breaking bifurcation of impulsively coupled oscillators," *Communications in Nonlinear Science and Numerical Simulation*, vol. 39, pp. 199–208, 2016.